Available online at www.sciencedirect.com
SCIENCE DIRECT®
Computers and Chemical Engineering 27 (2003) 1913–1924
Computers & Chemical Engineering
www.elsevier.com/locate/compchemeng

# Fault-tolerant control of fluid dynamic systems via coordinated feedback and switching

Nael H. El-Farra, Yiming Lou, Panagiotis D. Christofides *

*Department of Chemical Engineering, University of California, Los Angeles, CA 90095-1592, USA*

Received 3 April 2002; received in revised form 23 June 2003; accepted 24 June 2003

**Abstract**

This work addresses the problem of designing a fault-tolerant control system for fluid dynamic systems modeled by highly-dissipative partial differential equations (PDEs) with constrained control actuators. The proposed approach is predicated upon the idea of coordinating feedback controller synthesis and switching between multiple, spatially-distributed control actuator configurations. Using appropriate finite-dimensional approximations of the PDE system, a stabilizing feedback controller is designed for a given actuator configuration, and an explicit characterization of the constrained stability region is obtained. Switching laws are then derived, on the basis of these stability regions, to orchestrate the switching between the control actuator configurations, in a way that guarantees constraint satisfaction and preserves closed-loop stability of the infinite-dimensional system in the event of actuator failures. The results are demonstrated through an application of the proposed methodology to the suppression of wave formation in falling liquid films via the stabilization of the zero solution of the one-dimensional Kuramoto–Sivashinsky equation (KSE), with periodic boundary conditions, subject to actuator constraints and failures.
© 2003 Elsevier Ltd. All rights reserved.

*Keywords:* Highly-dissipative partial differential equations; Galerkin's method; Nonlinear bounded control; Switching actuator configurations; Input constraints; Kuramoto–Sivashinsky equation

## 1. Introduction

The development of general and practical control algorithms for nonlinear PDEs that describe fluid flow processes (e.g. Navier–Stokes equations, Kuramoto–Sivashinsky equation (KSE)) is a fundamental problem whose practical significance ranges from feedback control of turbulence for drag reduction, to suppression of fluid mechanical instabilities in coating processes and suppression of waves exhibited by falling liquid films. For example, drag reduction through active feedback control may have a significant impact on the design and operation of underwater vehicles, airplanes and automobiles since, according to some estimates, keeping the flow over the surface of a vehicle laminar could yield up to 30% reduction in fuel consumption. Active control of fluid flow can be achieved by injection of polymers, mass transport through porous walls (e.g. blowing/suction) and application of electro-magnetic forcing.

An example fluid dynamic system, which will be used throughout paper to demonstrate the results, is the KSE. The KSE is a nonlinear dissipative partial differential equation (PDE) of the form:

$$\frac{\partial U}{\partial t} = -\nu\frac{\partial^4 U}{\partial z^4} - \frac{\partial^2 U}{\partial z^2} - U\frac{\partial U}{\partial z} \tag{1}$$

where $\nu > 0$ is the so-called instability parameter, which describes incipient instabilities in a variety of physical and chemical systems, including falling liquid films (Chen & Chang, 1986), unstable flame fronts (Sivashinsky, 1980), Belouzov–Zabotinskii reaction patterns (Kuramoto & Tsuzuki, 1976) and interfacial instabilities between two viscous fluids (Hooper & Grimshaw, 1985). Both the dynamics and control of the KSE with periodic boundary conditions have been the subject of significant research work. Dynamical studies have led to the discoveries of steady and periodic wave solutions, chaotic behavior for very small values of $\nu$, and the

* Corresponding author.
*E-mail address:* pdc@seas.ucla.edu (P.D. Christofides).

0098-1354/03/$ - see front matter © 2003 Elsevier Ltd. All rights reserved.
doi:10.1016/S0098-1354(03)00161-3

fact that the dominant dynamics of the KSE can be adequately characterized, by a small number of degrees of freedom (see e.g. Temam, 1988; Chen & Chang, 1986; Greene & Kim, 1988; Kevrekidis, Nicolaenko & Scovel, 1990). Control studies of the KSE have focused on a variety of problems, including the design of finite-dimensional output feedback controllers for stabilization of the zero solution of the KSE based on ODE approximations (Armaou & Christofides, 2000), the global stabilization of the KSE via distributed static output feedback control (Christofides & Armaou, 2000), stabilization enhancement via boundary control (Liu & Krstic, 2001), adaptive stabilization (Kobayashi, 2002) and robust control (Hu & Temam, 2001).

While the above research efforts have led to a number of systematic approaches for control of the KSE and other fluid dynamic systems, a common theme of these approaches is the use of a fixed spatial arrangement (or configuration) of control actuators/measurement sensors in order to accomplish the desired control objectives. There are many practical situations, however, where it may be desirable and sometimes even necessary, to consider multiple actuator/sensor configurations and switch between them in a specific manner, in order to achieve the control objectives. One example is the problem of actuator failure where, upon the detection of a fault in a control actuator, it may be necessary to switch to an alternative actuator, placed at a different spatial location, in order to preserve stability of the closed-loop system. Spatially-distributed switching between control actuators in this case provides a means for fault-tolerant control. In other cases, switching between actuator configurations may be motivated by some additional performance objective, such as the desire to optimize a given performance criterion or accommodate inherently competing control objectives that cannot be reconciled using a single actuator configuration.

In previous works, we considered a class of linear (El-Farra & Christofides, 2003a) and quasi-linear (El-Farra & Christofides, 2003d) second-order parabolic PDE systems, and developed a method for handling control actuator failures by integrating feedback and switching among a pre-selected set of spatially-distributed control actuator configurations. The developed method, based on Lyapunov techniques, provides explicit feedback laws and precise switching conditions for guaranteeing closed-loop stability in the presence of actuator failures, and was successfully applied to representative examples of diffusion-reaction processes and a tubular reactor with recycle.

In the present work, we focus on the problem of coupling feedback and switching between actuator configurations for fault-tolerant control of fluid dynamic systems modeled by highly-dissipative PDEs with constrained control actuators. The results constitute a generalization of our previous work (El-Farra & Christofides, 2003a,d) to higher-order (e.g. fourth in the case of the KSE) dissipative PDEs that can model fluid flows. The problem is addressed on the basis of finite-dimensional Galerkin approximations of the PDE system and entails the integrated synthesis, via Lyapunov techniques, of stabilizing nonlinear feedback controllers together with stabilizing switching laws that orchestrate the switching between the admissible control actuator configurations, in a way that respects actuator constraints, accommodates inherently conflicting control objectives, and guarantees closed-loop stability. Precise conditions that guarantee stability of the constrained closed-loop system under switching are provided. The proposed control methodology is demonstrated through an application to the problem of suppression of wave formation, achieved via the stabilization of the zero solution, $U(z,\ t)=0$, of the KSE with periodic boundary conditions, in the presence of control actuator constraints and faults.

## 2. Preliminaries

### 2.1. Mathematical description

To demonstrate the proposed fault-tolerant control methodology, we consider the one-dimensional KSE with distributed control as our model system:

$$\frac{\partial U}{\partial t}=-\nu\frac{\partial^4 U}{\partial z^4}-\frac{\partial^2 U}{\partial z^2}-U\frac{\partial U}{\partial z}+\sum_{i=1}^{l} b_i u_i(t) \tag{2}$$

$$y_m^k=\int_{-\pi}^{\pi} s_k(z)U\,dz,\quad k=1,\ \ldots,\ p \tag{3}$$

subject to the periodic boundary conditions:

$$\frac{\partial^j U}{\partial z^j}(-\pi,\ t)=\frac{\partial^j U}{\partial z^j}(+\pi,\ t),\quad j=0,\ \ldots,\ 3 \tag{4}$$

and the initial condition:

$$U(z,\ 0)=U_0(z) \tag{5}$$

where $U(z,\ t)$ is the state of the system; $z\in[-\pi,\ \pi]$, the spatial coordinate; $t$, the time; $\nu$, the instability parameter; $u_i\in[-U_{\max},\ U_{\max}]\subset\mathbb{R}$, the $i$th constrained manipulated input; $l$, the total number of manipulated inputs; $b_i(z)$, the $i$th actuator distribution function (i.e. $b_i(z)$ determines how the control action computed by the $i$th control actuator; $u_i(t)$, is distributed (e.g. point or distributed actuation) in the spatial interval $[-\pi,\ \pi]$), $y_m^k\in\mathbb{R}$ denotes a measured output; and $s_k(z)$ is a known smooth function of $z$ which is determined by the location and type of the measurement sensors (e.g. point/distributed sensing). Whenever the control action enters the system at a single point $z_0$, with $z_0\in[-\pi,\ \pi]$ (i.e. point actuation), the function $b_i(z)$ is taken to be

nonzero in a finite spatial interval of the form $[z_0-\mu,\ z_0+\mu]$, where $\mu$ is a small positive real number, and zero elsewhere in $[-\pi,\ \pi]$.

For a precise presentation of our results, we cast the system of Eq. (2) as an infinite dimensional system in the Hilbert space $\mathscr{H}([-\pi,\ \pi];\mathbb{R})$, with $\mathscr{H}$ being the space of sufficiently smooth vector functions defined on $[-\pi,\ \pi]$ that satisfy the boundary condition of Eq. (4), with inner product and norm:

$$(\omega_1,\ \omega_2)=\int_{-\pi}^{\pi}(\omega_1(z),\ \omega_2(z))_{\mathbb{R}}dz,$$
$$\|\omega_1\|_2=(\omega_1,\ \omega_1)^{\frac{1}{2}} \tag{6}$$

where $\omega_1$, $\omega_2$ are two elements of $\mathscr{H}([-\pi,\ \pi];\mathbb{R})$ and the notation (-, -)$_{\mathbb{R}}$ denotes the standard inner product in $\mathbb{R}$.

Defining the state function $x$ on $\mathscr{H}([-\pi,\ \pi];\mathbb{R})$ as:

$$x(t)=U(z,\ t),\quad t>0,\ \ z\in[-\pi,\ \pi], \tag{7}$$

the operator $\mathscr{A}$ in $\mathscr{H}([-\pi,\ \pi];\mathbb{R})$ as:

$$\mathscr{A}x=-\nu\frac{\partial^4 U}{\partial z^4}-\frac{\partial^2 U}{\partial z^2},$$
$$x\in\mathscr{D}(\mathscr{A})$$
$$=\left\{x\in\mathscr{H}([-\pi,\ \pi];\mathbb{R}):\frac{\partial^j U}{\partial z^j}(-\pi,\ t)=\frac{\partial^j U}{\partial z^j}(+\pi,\ t),\right. \tag{8}$$
$$\left.j=0,\ \ldots,\ 3\right\}$$

and the input, and measured output operators as:

$$\mathscr{B}u=\sum_{i=1}^{l}b_i u_i,\qquad \mathscr{S}x=(s,\ x) \tag{9}$$

the system of Eqs. 2–5 takes the form:

$$\dot{x}=\mathscr{A}x+\mathscr{B}u+f(x),\qquad x(0)=x_0$$
$$y_m=\mathscr{S}x \tag{10}$$

where $f(x(t))=-U(\partial U/\partial z)$ and $x_0=U_0(z)$.

For $\mathscr{A}$, we can formulate the following eigenvalue problem:

$$\mathscr{A}\bar{\phi}_n=-\nu\frac{\partial^4\bar{\phi}_n}{\partial z^4}-\frac{\partial^2\bar{\phi}_n}{\partial z^2}=\lambda_n\bar{\phi}_n,\quad n=1,\ \ldots,\ \infty \tag{11}$$

subject to:

$$\frac{\partial^j\bar{\phi}_n}{\partial z^j}(-\pi)=\frac{\partial^j\bar{\phi}_n}{\partial z^j}(+\pi),\quad j=0,\ldots,\ 3 \tag{12}$$

where $\lambda_n$ denotes an eigenvalue and $\bar{\phi}_n$ denotes an eigenfunction of $\mathscr{A}$ (the notation $\bar{\phi}_n$ denotes all the eigenvalues of $\mathscr{A}$ including $\psi_0$, $\psi_n$, $\phi_n$ which are given below). A direct computation of the solution of the above eigenvalue problem yields $\lambda_0=0$ with $\psi_0(z)=1/\sqrt{2\pi}$ and $\lambda_n=-\nu n^4+n^2$ ($\lambda_n$ is an eigenvalue of multiplicity two) with eigenfunctions $\phi_n(z)=(1/\sqrt{\pi})\sin(nz)$ and $\psi_n(z)=(1/\sqrt{\pi})\cos(nz)$ for $n=1,\ \ldots,\ \infty$. We also define the eigenspectrum of $\mathscr{A}$, $\sigma(\mathscr{A})$, as the set of all eigenvalues of $\mathscr{A}$, i.e. $\sigma(\mathscr{A})=\{\lambda_1,\ \lambda_2,\ \ldots\}$. We note that the fact that $\mathscr{A}$ has a pure real point spectrum is a result of the fact that the linear part of the spatial differential operator of the KSE with periodic boundary conditions is self-adjoint and the problem is considered in a bounded domain.

From the expression of the eigenvalues, it follows that, for a fixed value of $\nu>0$, the number of unstable eigenvalues of $\mathscr{A}$ is finite and the distance between two consecutive eigenvalues (i.e. $\lambda_n$ and $\lambda_{n+1}$) increases as $n$ increases. Furthermore, for a fixed value of $\nu>0$, $\sigma(\mathscr{A})$ can be partitioned as $\sigma(\mathscr{A})=\sigma_1(\mathscr{A})\bigcup\sigma_2(\mathscr{A})$, where $\sigma_1(\mathscr{A})$ contains the first $m$ (with $m$ finite) "slow" eigenvalues (i.e. $\sigma_1(\mathscr{A})=\{\lambda_1,\ \ldots,\ \lambda_m\}$) and $\sigma_2(\mathscr{A})$ contains the remaining "fast" eigenvalues (i.e. $\sigma_2(\mathscr{A})=\{\lambda_{m+1},\ \ldots\}$ where $\lambda_{m+1}<0$). To capture the separation between the "slow" and "fast" eigenvalues, we define the parameter $\epsilon=|\lambda_1|/|\lambda_{m+1}|$ (note that $\epsilon\to0$ as $m\to\infty$). The separation between the "slow" and "fast" eigenvalues suggests that the dominant dynamics of the KSE can be described by a finite-dimensional system and motivates applying Galerkin's method to the system of Eq. (10) to derive an approximate finite-dimensional system (see Section 3.1 below).

*Remark 1*. A physical system that can be described by the KSE is the motion of a liquid film falling down on a vertical wall (Chen & Chang, 1986). In this case, $U(z,t)$ is the film height. Such a system has been found experimentally to exhibit wavy behavior of the type predicted by the KSE for values of $\nu$ smaller than 1 (see also Fig. 2). In many instances, it is desirable to suppress wavy behavior by using control actuators that add/remove fluid mass via blowing/suction. In this case, the control input enters directly into the PDE and does not appear in the boundary conditions. This physical problem is consistent with the formulation of Eq. (2) since we consider distributed control actuation. Note that problems for which the inputs enter directly into the KSE but nonlinearly can be readily handled within our formulation by simply solving for $u$ through the inversion of a nonlinear algebraic equation.

*Remark 2*. The consideration of approximate point control is motivated by the fact that most experimental point control actuators (including the ones that add/remove fluid mass via blowing/suction) have finite (but small) support and the fact that $b_i(z)=\delta(z-z_0)$ (where $\delta(\cdot)$ is the standard Dirac function) is not an element, of $\mathscr{H}([-\pi,\ \pi];\mathbb{R})$.

### 2.2. Problem formulation

Consider the system of Eq. (2), where the manipulated inputs $u_i$ are constrained in the interval $[-U_{\max}, U_{\max}]$ and assume that available at our disposal is a family of $N$ (with $N$ finite) control actuator configurations, of which only one configuration can be used for control at any given time instance. Each of these $N$ configurations consists of a spatially-distinct arrangement of the control actuators, which we denote by $\bar{z}_{k(t)}$, $k=1, \ldots, N$. In this notation, the index $k(t)$ denotes the actuator configuration being active at time $t$, while $\bar{z}_k$ is a column vector whose components represent the corresponding spatial locations of the actuators associated with the $k$th configuration. To ensure controllability of the system, we allow only a finite number of switches between configuration over finite time. The problem is how to coordinate switching between the different control actuator configurations, in the event of actuator failure, in a way that respects actuator constraints and guarantees closed-loop stability. To address this problem, we formulate the following objectives. Initially, Galerkin's method is used to derive a nonlinear finite-dimensional ODE system that captures the dominant dynamics of the KSE. Next, the ODE approximation is used as the basis for the synthesis of bounded nonlinear output feedback controllers of the general form:

$$u = p(y_m,\ u_{\max},\ \bar{z}_k) \tag{13}$$

that enforce asymptotic stability and reference-input tracking in the constrained closed-loop system and provide an explicit characterization of the stability region, associated with each control actuator configuration. The controller synthesis is carried out via Lyapunov-based control techniques and is inspired by the results on bounded control in Lin and Sontag (1991). Finally, a set of switching rules is derived to determine which of the $N$ control actuator configurations can be engaged at any given time, and an upper bound on the separation between the slow and fast eigenvalues, which guarantees stability of the closed-loop infinite-dimensional system, is computed.

## 3. Fault-tolerant control system design

### 3.1. Galerkin's method

We apply Galerkin's method to the system of Eq. (10) to derive an approximate finite-dimensional system. Let $\mathscr{H}_s$, $\mathscr{H}_f$ be modal subspaces of $\mathscr{A}$, defined as $\mathscr{H}_s = span\{\bar{\phi}_1, \bar{\phi}_2, \ldots, \bar{\phi}_m\}$ and $\mathscr{H}_f = span\{\bar{\phi}_{m+1}, \bar{\phi}_{m+2}\}$ (the existence of $\mathscr{H}_s$, $\mathscr{H}_f$ follows from the properties of $\mathscr{A}$). Defining the orthogonal projection operators $\mathscr{P}_s$ and $\mathscr{P}_f$ such that $x_s = \mathscr{P}_s x$, $x_f = \mathscr{P}_f x$, the state $x$ of the system of Eq. (10) can be decomposed as:

$$x = x_s + x_f = \mathscr{P}_s x + \mathscr{P}_f x \tag{14}$$

Applying $\mathscr{P}_s$ and $\mathscr{P}_f$ to the system of Eq. (10) and using the above decomposition for $x$, the system of Eq. (10) can be equivalently written in the following form:

$$\frac{dx_s}{dt} = \mathscr{A}_s x_s + \mathscr{B}_s u + f_s(x_s,\ x_f)$$

$$\frac{\partial x_f}{\partial t} = \mathscr{A}_f x_f + \mathscr{B}_f u + f_f(x_s,\ x_f)$$

$$y_m = \mathscr{S} x_s + \mathscr{S} x_f$$

$$x_s(0) = \mathscr{P}_s x(0) = \mathscr{P}_s x_0, \qquad x_f(0) = \mathscr{P}_f x(0) = \mathscr{P}_f x_0 \tag{15}$$

where $\mathscr{A}_s = \mathscr{P}_s \mathscr{A}$, $\mathscr{B}_s = \mathscr{P}_s \mathscr{B}$, $f_s = \mathscr{P}_s f$, $\mathscr{A}_f = \mathscr{P}_f \mathscr{A}$, $\mathscr{B}_f = \mathscr{P}_f \mathscr{B}$ and $f_f = \mathscr{P}_f f$ and the partial derivative notation in $(\partial x_f/\partial t)$ is used to denote that the state $x_f$ belongs in an infinite-dimensional space. In the above system, $\mathscr{A}_s$ is a diagonal matrix of dimension $m \times m$ of the form $\mathscr{A} = diag\{\lambda_j\}$, $f_s(x_s,\ x_f)$ and $f_f(x_s,\ x_f)$ are Lipschitz vector functions, and $\mathscr{A}_f$ is an unbounded differential operator which is exponentially stable (following from the fact that $\lambda_{m+1} < 0$ and the selection of $\mathscr{H}_s$, $\mathscr{H}_f$). Neglecting the fast and stable infinite-dimensional $x_f$-subsystem in the system of Eq. (15), the following $m$-dimensional slow system is obtained:

$$\frac{d\tilde{x}_s}{dt} = \mathscr{A}_s \tilde{x}_s + \mathscr{B}_s u + f_s(\tilde{x}_s,\ 0)$$

$$\tilde{y}_m = \mathscr{S} \tilde{x}_s \tag{16}$$

where the tilde symbol in $\tilde{x}_s$ and $\tilde{y}_m$ denotes that these variables are associated with a finite-dimensional system.

### 3.2. Coordinating feedback and switching

Having obtained a finite-dimensional model that describes the dominant dynamics of the KSE, we proceed in this section to describe the proposed procedure for designing the fault-tolerant control system, on the basis of the finite-dimensional approximation in Eq. (16). To this end, and since our objective is the stabilization of the zero solution of the KSE, we define the controlled outputs as the slow modes of the KSE, and assume, for simplicity, that the number of inputs is equal to the number of slow modes. Though not discussed in this paper explicitly, the results can be generalized to address the problem of reference-input tracking. With this in mind, the slow modes of the KSE can be described by the following $m$-dimensional system:

$$\dot{a}_s(t) = F a_s(t) + \bar{G}(\bar{z}_k) u(t) + \tilde{f}(a_s(t)) \tag{17}$$

where $a_s(t) = [a_1(t), \ldots, a_m(t)]^T \in \mathbb{R}^m$, $a_i(t)$ is the

amplitude of the $i$th eigenmode, $\tilde{x}_s(t) = \Sigma_{j=1}^{m} a_j(t)\bar{\phi}_j(z)$, $(x_s(t), \bar{\phi}_j) = a_j(t)(\bar{\phi}_j, \bar{\phi}_j)$, $F$ is an $m \times m$ diagonal matrix of the form $F = diag\{\lambda_j\}$, $\bar{G}$ is an $m \times$ m matrix whose $(i, k)$th element is given by $\bar{G}_{ik} = \bar{\phi}(\bar{z}_k)$, and $\tilde{f}(\cdot)$ is a nonlinear, locally Lipschitz function of its argument. Finally, we define $\bar{f}(a_s) = Fa_s + \tilde{f}(a_s)$ and denote by $\bar{g}_i$ the $i$th column of the matrix $\bar{G}$.

The design procedure consists of three basic steps. These include: (1) the synthesis of a stabilizing feedback controller; (2) the characterization of the constrained stability region associated with each control actuator configuration; and (3) the design of a switching law that orchestrates the re-configuration of control actuators in a way that guarantees closed-loop stability in the event of actuator failure. Below is a brief description of each step.

### 3.2.1. Feedback controller synthesis

The first step in designing the fault-tolerant control system is to synthesize a feedback controller that enforces closed-loop stability in the presence of input constraints. This task is carried out on the basis of the finite-dimensional slow system of Eq. (17) using Lyapunov techniques. In particular, using a quadratic Lyapunov function of the form $V = a_s^T \Phi a_s$, where $\Phi$ is a positive-definite symmetric matrix that satisfies the inequality $F^T\Phi + \Phi F - \Phi\bar{G}\bar{G}^T\Phi < 0$, we synthesize the following bounded nonlinear feedback law (the detailed calculations for controller synthesis and the construction of the stability region can be found in El-Farra and Christofides, 2003b):

$$u = -r(a_s, u_{\max}^k, \bar{z}_k)(L_{\bar{G}}V)^T(\bar{z}_k) \tag{18}$$

where

$$r(a_s, u_{\max}^k, \bar{z}_k) = \frac{L_f^* V + \sqrt{(L_f^* V)^2 + (u_{\max}^k |(L_{\bar{G}}V)^T(\bar{z}_k)|)^4}}{|(L_{\bar{G}}V)^T(\bar{z}_k)|^2[1 + \sqrt{1 + (u_{\max}^k |(L_{\bar{G}}V)^T(\bar{z}_k)|)^2}]} \tag{19}$$

where $\bar{z}_k = [\bar{z}_{k_1}, \bar{z}_{k_2}, \ldots, z_{k_m}]^T$, $k = 1, \ldots, N$, $L_f^* V = L_{\bar{f}}V + \rho|a_s|^2$, $\rho > 0$, $L_{\bar{G}}V$ is a row vector of the form $[L_{\bar{g}_1}V \ldots L_{\bar{g}_m}V]$. The notation $u_{\max}^k$ is used to indicate the magnitude of actuator constraints associated with the $k$th configuration. This number is allowed to vary from one configuration to another. The scalar function $r(\cdot)$ in Eqs. 18–19 can be thought of as a nonlinear controller gain. This Lyapunov-based gain, which depends on both the magnitude of actuator constraints, $u_{\max}^k$, and the actuator configuration used, $\bar{z}_k$, is shaped in a way that guarantees constraint satisfaction and asymptotic closed-loop stability within a well-characterized region in the state space. The characterization of this region is discussed in the next step.

### 3.2.2. Characterization of stability regions

Given that actuator constraints place fundamental limitations on both the initial conditions and actuator locations that can be used for stabilization, it is important for the control system designer to explicitly characterize these limitations by identifying, for each actuator configuration, the set of feasible initial conditions starting from where the constrained closed-loop system is asymptotically stable. As will be discussed in step 3 below, this characterization is necessary for the design of an appropriate switching scheme that ensures fault-tolerance. The control law designed in step 1 provides such a characterization. Specifically, for this control law, one can show (see El-Farra & Christofides, 2003b for a detailed proof) that the set described by:

$$\Theta(u_{\max}^k, \bar{z}_k) = \{a_s \in \mathbb{R}^m : L_f^* V \le u_{\max}^k |(L_{\bar{G}}V)^T(\bar{z}_k)|\} \tag{20}$$

represents a set where the control action satisfies the constraints and the time-derivative of the Lyapunov function is negative-definite along the trajectories of the closed-loop system of Eq. (17). Note that the size of this set depends, as expected, on the magnitude of the constraints. In particular, the set becomes smaller as the constraints become tighter (smaller $u_{\max}^k$). Note also that the set $\Theta(u_{\max}^k, \bar{z}_k)$ is parameterized by the actuator locations because the matrix $\bar{G}$ in Eq. (17) depends on the actuator locations. Therefore, for a given actuator configuration (fixed $\bar{z}_k$), one can use the above inequality to estimate the stability region associated with this configuration. This is done by constructing the largest invariant subset of $\Theta$, which we denote by $\Omega(u_{\max}^k, \bar{z}_k)$. Confining the initial conditions within the set $\Omega(u_{\max}^k, \bar{z}_k)$ ensures that the closed-loop trajectory stays within the region defined by $\Theta(u_{\max}^k, \bar{z}_k)$, and thereby $V$ continues to decay monotonically, for all times that the $k$th actuator configuration is active.

### 3.2.3. Switching logic for actuator re-configuration

Having designed the feedback control law in step 1, and characterized the stability region associated with each actuator configuration in step 2, the final step in the control system design procedure is to derive a switching rule that orchestrates the re-configuration of the control actuators in the event of actuator failure. This rule determines which of the backup actuator configurations can be activated, in the event of actuator failure, in order to preserve closed-loop stability. The need for a switching rule stems from the fact that even if the controller enforces closed-loop stability for each actuator configuration individually, closed-loop stability of the switched system is not guaranteed unless restrictions are placed on the switching logic. In particular, owing to the limitations imposed by input constraints on the stability region for each actuator configuration, switching from the current malfunction-

ing actuator configuration to a well-functioning, but arbitrarily selected, backup configuration will not help preserve closed-loop stability if the state of the system, at the time of actuator failure, lies outside the stability region of the chosen backup configuration. In this case, stabilization using this configuration would require more control action than is allowed by its constraints. This observation underscores the main idea of the proposed switching logic, which is to switch to the actuator configuration for which the closed-loop state resides within the stability region at the time of actuator failure. Without loss of generality, let the initial actuator configuration be $k(0)=1.$ and let $T$ be the time when this configuration fails, then the switching rule given by:

$$k(T)=j \quad \text{if} \quad a_s(T)\in\Omega(u^j_{\max},\ \bar{z}_j), \qquad j\in\{2,\ 3,\ \ldots,\ N\} \tag{21}$$

guarantees closed-loop asymptotic stability. The implementation of the above switching law requires monitoring the closed-loop state trajectory with respect to the stability regions associated with the various actuator configurations.

*Remark 3*. While the fault-tolerant control approach outlined above has been developed on the basis of the finite-dimensional system of Eq. (17), the large separation between the slow and fast eigenmodes of the spatial differential operator of the KSE allows the application of this approach to the infinite-dimensional system. In particular, one can show (using the singular perturbation formulation of Galerkin's method; see Christofides, 2001) that the proposed feedback and switching scheme guarantees asymptotic closed-loop stability for the infinite-dimensional system of Eq. (2), provided that $\epsilon$ is sufficiently small. Note that from the definition of $\epsilon$, it follows that $\epsilon\to 0$ as $m\to\infty$, which implies that stability of the infinite-dimensional closed-loop system is guaranteed provided that $m$ is sufficiently large. Even though an estimate of how small $\epsilon$ needs to be can, in principle, be obtained using singular perturbation methods, such an estimate may be conservative in general and, therefore, the appropriate number of slow modes is usually tested via closed-loop simulations.

*Remark 4*. The stability region associated with each set of actuators is derived on the basis of the approximate ODE model that describes the evolution of the slow modes (with the fast modes neglected). This region describes the set of initial slow states starting from where the reduced-order model can be stabilized for a given set of constrained control actuators. Due to the error introduced by neglecting the fast modes, this region is not exactly the same as the set of initial slow states starting from where the full system can be stabilized. However, if the separation between the slow and fast modes is large enough, the stability region of the approximate system will approach that of the slow part of the full system. The discrepancy between the two regions can be made small by including additional modes in constructing the reduced-order model. Alternatively, for a given choice of the order of the approximation (that is adequate for stabilization), one can treat the effect of the fast states as a disturbance to the approximate slow system and use this to further constrain the size of the nominal stability region originally derived by neglecting the fast states (e.g. see El-Farra & Christofides, 2003b for a discussion on the construction of stability regions for constrained nonlinear systems with disturbances).

*Remark 5*. The control objective in this work is to achieve fault-tolerant stabilization of the infinite-dimensional system without using an unnecessarily large number of control actuators. Therefore, from a stability point of view, only a small set (depending on the value of $v$) of well-functioning control actuators is needed at any given time to ensure closed-loop stability (which is equal to the number of slow modes being controlled). From a performance standpoint, however, the use of multiple sets of actuators at a given time, simultaneously, could be useful. On the other hand, this can increase the total cost of control implementation and may not always yield appreciable performance improvement. Furthermore, the simultaneous use of multiple actuator sets, to improve performance, may not be feasible in some cases due to the fundamental limitations of actuator constraints that restrict the stability region of each actuator set. Therefore, even though a given set of actuators may be non-failing, it may not be possible to use the actuators of that set at a given time if, at this time, the state of the system is outside the corresponding stability region. Using this set in conjunction with the set of operating actuators may in fact lead to instability (see Section 4 for examples).

*Remark 6*. Due to the spatially-distributed nature of the KSE control problem, the switching scheme proposed in this paper differs from the schemes proposed in hybrid controller design for lumped-parameter systems. For lumped systems, with no spatial variation, the idea is to achieve the control objectives by switching between members of an a priori specified family of feedback functions, whereas in the approach that we follow in this work, we seek to achieve the control objectives by switching between members of an a priori specified family of spatially-distributed control actuator configurations, using the same feedback function (parameterized by $\bar{z}_k$). The area of switched and hybrid controller design for lumped systems is currently an active area of research (e.g. see Bemporad & Morari, 1999; Liberzon & Morse, 1999; El-Farra & Christofides, 2003c and the references therein for results in this area).

*Remark 7*. Under the assumption that the number of measurements is equal to the number of slow modes and that the inverse of the operator $\mathcal{S}$ exists (which can be

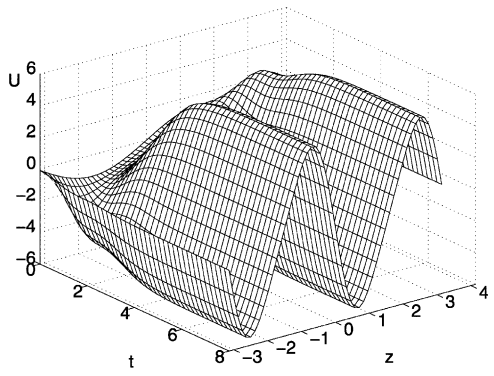


Fig. 1. Open-loop spatiotemporal profile of $U(z, t)$ for $\nu = 0.2$.

ensured via appropriate selection of the measurement sensors' locations), an output feedback controller can be designed by combining the state feedback controller of Eqs. 18–19 with an estimator that provides estimates for the states of the approximate ODE model of Eq. (16) from the measurements. While the estimation error leads to some loss in the size of the stability region obtained under state feedback, this loss can be made small by increasing the order of the ODE approximation and including more measurements. This approach, therefore, allows us to asymptotically (as $\epsilon \to 0$) recover the state feedback stability region associated with each control actuator configuration.

## 4. Simulation results

In this section, we demonstrate how the integrated feedback and switching scheme outlined in Section 3.2 can be used to deal with the problem of actuator failure, in the context of stabilizing the zero solution of the one-dimensional KSE with periodic boundary conditions and input constraints. For simplicity, we will consider the KSE in the space of odd functions with spatial zero mean. Introducing the Hilbert space $\mathscr{H}$ of sufficiently smooth odd functions that satisfy the boundary conditions of Eq. (4) and have spatial zero mean (i.e. $\forall \omega \in \mathscr{H}$, $\int_{-\pi}^{\pi} \omega(z)dz = 0$) and defining the state function $x \in \mathscr{H}$ as $x(t) = U(z, t)$, $\forall z \in [-\pi, \pi]$, the system of Eqs. 2–5 can be written in the form of Eq. (10), where the domain of definition of the spatial differential operator $\mathscr{A}$ now takes the form:

$$x \in \mathscr{D}(\mathscr{A}) = \left\{ x \in \mathscr{H}([-\pi,\ \pi];\ \mathbb{R});\ \frac{\partial^j U}{\partial z^j}(-\pi,\ t) = \frac{\partial^j U}{\partial z^j}(\pi,\ t),\ j = 0,\ \ldots,\ 3 \right\} \quad (22)$$

and the eigenvalue problem for $\mathscr{A}$ yields $\lambda_j = -\nu_j^4 + j^2$, $\phi_j(z) = \sqrt{1/\pi}\sin(jz)$, $j = 1,\ \ldots,\ \infty$ (note that $\psi_0(z) = \sqrt{1/2\pi}$ and $\psi_j(z) = \sqrt{1/\pi}\cos(jz)$ $j = 1,\ \ldots,\ \infty$ are not considered here since we focus only on odd functions with spatial zero mean).

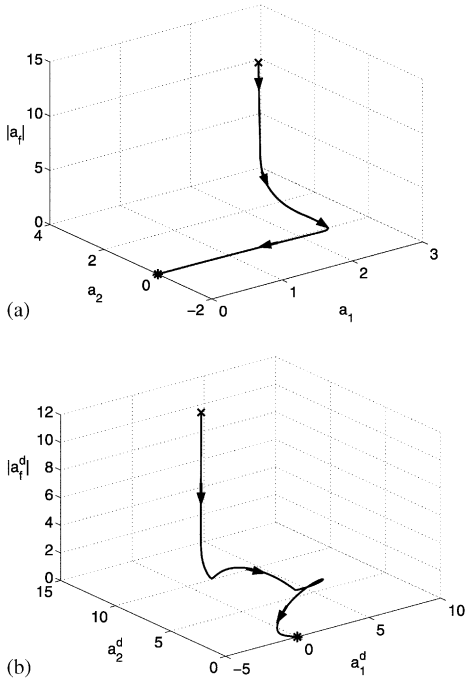


Fig. 2. (a) Evolution of the norm of the fast modes, $a_f = [a_3, \ldots, a_{30}]$, and of the two dominant modes, $a_1$ and $a_2$, for $\nu = 1.2$. (b) Evolution of the norm of the fast modes (in deviation variable form), $a_f^d = [a_3^d, \ldots, a_{30}^d]$, and of the two dominant modes, $a_1^d$ and $a_2^d$, for $\nu = 0.2$ (all modes are in deviation variable form).

Linearizing the system around the spatially uniform steady-state, we observe that, for $\nu = 0.2$, the system possesses two unstable eigenvalues. Using a 30th order Galerkin discretization of the KSE, we simulate the open-loop system with $\nu = 0.2$ (higher-order discretizations led to identical results). The resulting spatiotemporal evolution of $U(z, t)$ is depicted in Fig. 1 and clearly shows that the spatially uniform steady-state, $U(z, t) = 0$, is unstable for $\nu = 0.2$. The control objective, therefore, is to stabilize the system at this unstable steady-state. To achieve this objective, we consider the first two eigenvalues to be the dominant ones and use standard Galerkin's method to derive the following second-order model (to be used for controller design) that describes the temporal evolution of the amplitudes of the first two eigenmodes:

$$\begin{bmatrix} \dot{a}_1(t) \\ \dot{a}_2(t) \end{bmatrix} = \begin{bmatrix} \lambda_1 & 0 \\ 0 & \lambda_2 \end{bmatrix} \begin{bmatrix} a_1(t) \\ a_2(t) \end{bmatrix} + \begin{bmatrix} \phi_1(\bar{z}_1) & \phi_1(\bar{z}_2) \\ \phi_2(\bar{z}_1) & \phi_2(\bar{z}_2) \end{bmatrix} \begin{bmatrix} u_1 \\ u_2 \end{bmatrix} + \begin{bmatrix} f_1(a_1,\ a_2) \\ f_2(a_1,\ a_2) \end{bmatrix} \quad (23)$$

where $(\dot{\bar{x}}_s,\ \phi_i) = a_i(t)(\phi_i,\ \phi_i)$, $i = 1,\ 2$. $\bar{z}_1$ and $\bar{z}_2$ are the locations of the two point actuators used for stabilization. The explicit forms of the terms $f_1(a_1, a_2)$ and $f_2(a_1, a_2)$ are omitted for brevity. The system of Eq. (23) is

derived by assuming that point actuation is applied to the system. When the point actuation is approximated by a control action applied to a small spatial interval, the closed-loop simulation results are almost identical to those obtained by using the system of Eq. (23). Before proceeding with controller synthesis on the basis of the above system, we first demonstrate that the first two modes indeed capture the dominant dynamics of the nonlinear KSE. To this end, we simulate the open-loop system, using the high (30th) order Galerkin discretization, for two values of the instability parameter, $\nu = 1.2$ and 0.2. For each value, we plot the norm of the vector of "fast" modes, $a_f = [a_3 \ldots a_{30}]$ and the amplitude of the first two modes on a three-dimensional plot. The results are shown in Fig. 2, where the top plot shows the result for $\nu = 1.2$ (where the zero steady-state is globally asymptotically stable), while the bottom plot shows the result for $\nu = 0.2$ (where the zero steady-state is unstable and the system moves to a spatially non-uniform steady-state; see Fig. 1). In the bottom plot, for convenience, the results are presented in terms of the deviation from the stable, spatially non-uniform steady-state in order to shift the equilibrium state to the origin, i.e. $a_f^d = [a_3^d \ldots a_{30}^d]$ where $a_i^d = a_i - a_{i,s}$, $i = 3, \ldots, 30$, and $a_{i,s}$ is the steady-state value of the $i$th mode that corresponds to the spatially non-uniform stable steady-state of the KSE with $\nu = 0.2$. In both plots, it is clear that the dynamics of the high-order system converge quickly to the subspace described by the first two modes, implying that the first two modes are the dominant ones. In particular, note that the norm of the modes $a_f = [a_3 \ldots a_{30}]$ drops quickly to zero and that beyond this point the entire system evolution is basically captured by the evolution of the first two modes. These results motivate the use of the system of Eq. (23) for the synthesis of the controller, using Eqs. 18–19, and the switching law, using Eqs. 20–21. The controller and switching laws are then implemented on a high-order Galerkin discretization (30th order) of the nonlinear KSE (further increase in the order of the approximation led to identical results). The closed-loop high-order system is then integrated numerically, forward in time, using explicit Euler method.

To illustrate different aspects of the proposed fault-tolerant control scheme, we consider the following two problems where switching is needed to preserve closed-loop stability. In the first problem, two pairs of point control actuators, placed at ($\bar{z}_1 = 0.3\pi$, $\bar{z}_2 = 0.7\pi$) (configuration A) and ($\bar{z}_1 = 0.1\pi$, $\bar{z}_2 = 0.9\pi$) (configuration B) are assumed to be available. Both pairs have the same constraints of $u_{\max}^A = u_{\max}^B = 2.0$, but only one configuration can be used for control at any given moment. The question to be addressed here is: when is it feasible to switch to configuration B given that a fault is detected in the actuators of configuration A. In the second problem, we assume that a third pair of actuators,

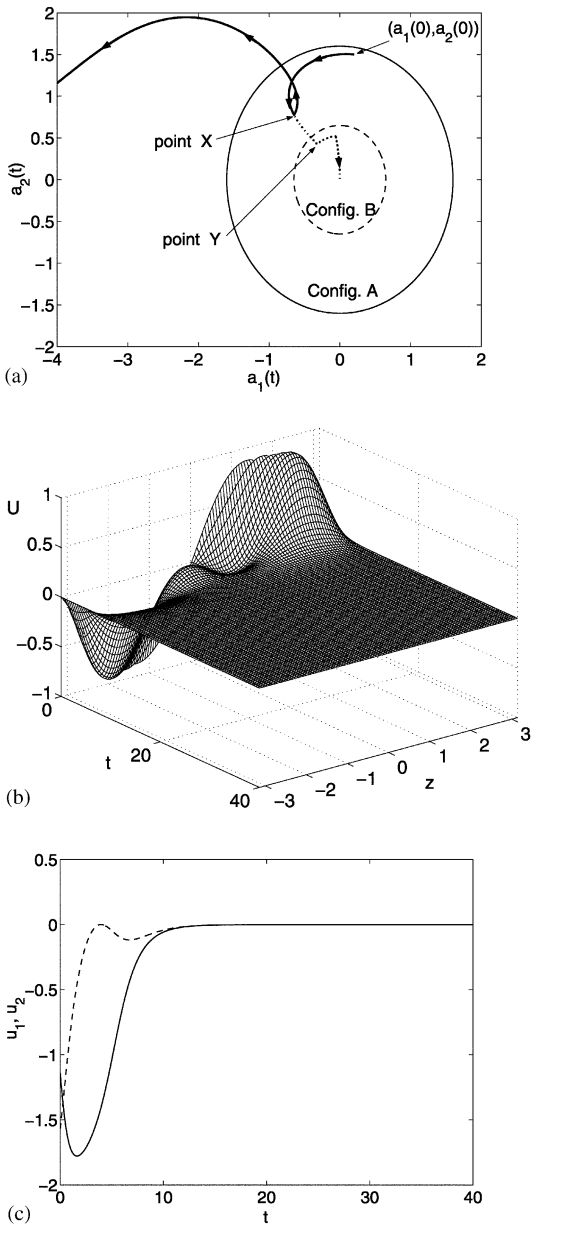


Fig. 3. (a) Stability regions for configuration A ($u_{\max} = 2.0$, $z_1 = 0.3\pi$, $z_2 = 0.7\pi$) (solid ellipse) and for configuration B ($u_{\max} = 2.0$, $z_1 = 0.1\pi$, $z_2 = 0.9\pi$) (dashed ellipse). (b) Closed-loop state profile (state feedback) for $(a_1(0), a_2(0)) = (0.2, 1.5)$ using configuration A without switching. (c) Corresponding manipulated input profiles for $u_1$ (solid) and $u_2$ (dashed).

located at ($\bar{z}_1 = 0.2\pi$, $\bar{z}_2 = 0.8\pi$) (configuration C) with constraints of $u_{\max}^C = 0.5$ is also available (in addition to configurations A and B). Again, only one of the three configurations can be active at any given moment. The problem here is to decide which of the two "fall-back" actuator configurations (B or C) should be activated, once the actuators of configuration A fail. Basically, the first problem deals with the issue of identifying the appropriate switching times for a fixed re-configuration strategy, while the second problem addresses the issue of

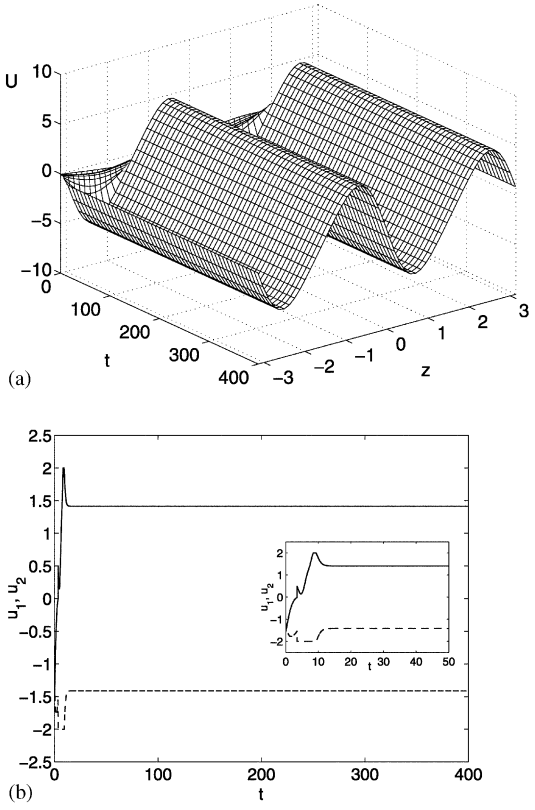


Fig. 4. (a) Closed-loop state profile (state feedback) for $(a_1(0), a_2(0)) = (0.2, 1.5)$ when configuration A fails at $t = 3.5$ and configuration B is activated. (b) Corresponding manipulated input profiles for $u_1$ (solid) and $u_2$ (dashed).

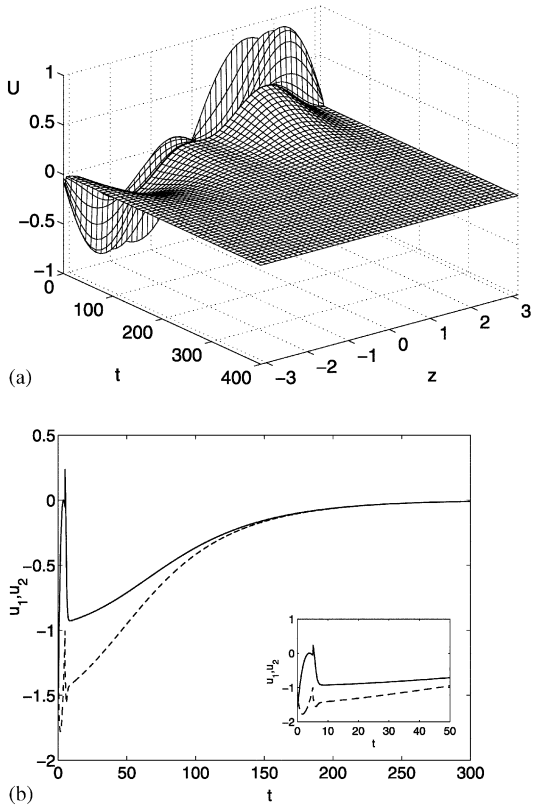


Fig. 5. (a) Closed-loop state profile (state feedback) for $(a_1(0), a_2(0)) = (0.2, 1.5)$ when configuration A fails at $t = 5$ and configuration B is activated. (b) Corresponding manipulated input profiles for $u_1$ (solid) and $u_2$ (dashed).

how to select the appropriate actuator re-configuration strategy among a family of possible choices, in order to provide the necessary fault-tolerance.

The simulation results under state feedback control are presented first. For the first problem, we initially use Eq. (20) with $\rho = 0.001$ to compute the stability regions for configurations A and B. To simplify the presentation of our results, we show in Fig. 3a the set of admissible initial conditions for the amplitudes, $a_1(0)$ and $a_2(0)$, of the first two eigenmodes, respectively, for configuration A (solid ellipse) and configuration B (dashed ellipse) (note that $x_s(0) = a_1(0)\phi_1(z) + a_2(0)\phi_2(z)$). From this figure, it is clear that for an initial condition $(a_1(0), a_2(0)) = (0.2, 1.5)$, only configuration A can be used initially since the initial condition is outside the stability region for configuration B. Fig. 3b–c depict, respectively, the closed-loop state and manipulated input profiles corresponding to this initial condition and using configuration A. Clearly, the controller successfully stabilizes the KSE at the desired steady-state. Now, suppose that sometime after starting from this initial condition, a fault is detected in configuration A. From Fig. 3a, we see that switching to configuration B may or may not solve the problem depending on when the failure of A actually occurs. For example, consider the case when A fails at $t = 3.5$. By monitoring the slow state evolution over time, we find that the state is outside the stability region for B at this time, as shown by point X on the solid trajectory in Fig. 3a. Therefore, switching to configuration B will not preserve closed-loop stability (note that the solid trajectory settles at another steady-state after switching at point X). This is also confirmed by the unstable closed-loop state profile in Fig. 4a. The corresponding profiles for both manipulated inputs are shown in Fig. 4b which show that the inputs stay saturated. Suppose now that configuration A fails at $t = 5$. In this case, we see from the dashed trajectory in Fig. 3a that the state at this time is within the stability region for configuration B (point Y) and, according to our switching scheme, closed-loop stability can be maintained by switching to configuration B at this time (note that the dashed trajectory in Fig. 3a converges to the origin when configuration B is activated at point Y). This is also demonstrated in Fig. 5 which shows that the controller successfully stabilizes the KSE when configuration B is activated at $t = 5$.

We now turn our attention to the second problem. The stability regions for configurations A, B, and C are depicted in Fig. 6a by the solid, dashed, and dotted ellipses, respectively. From this figure, it is easy to see

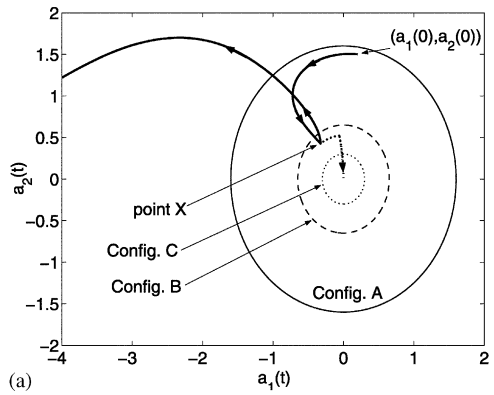


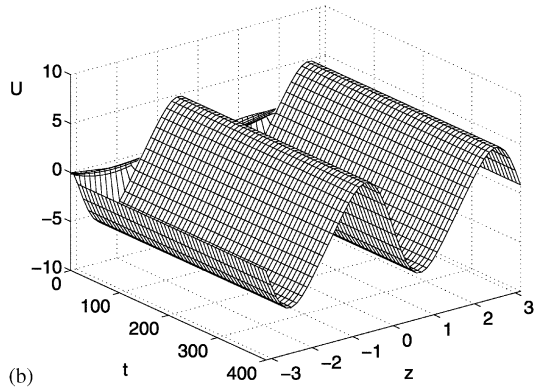


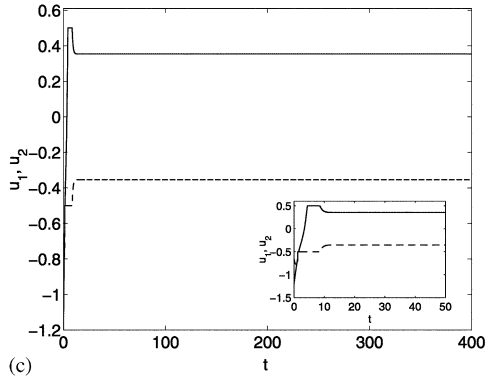


Fig. 6. (a) Stability regions for configuration A ($u_{max} = 2.0$, $z_1 = 0.3\pi$, $z_2 = 0.9\pi$) (solid ellipse); configuration B ($u_{max} = 2.0$, $z_1 = 0.1\pi$, $z_2 = 0.9\pi$) (dashed ellipse), and configuration C ($u_{max} = 0.5$, $z_1 = 0.2\pi$, $z_2 = 0.8\pi$). (b) Closed-loop state profile (state feedback) for $(a_1(0), a_2(0)) = (0.2, 1.5)$ when configuration A fails at $t = 3.5$ and configuration C is activated. (b) Corresponding manipulated input profiles for $u_1$ (solid) and $u_2$ (dashed).

that for the initial condition $(a_1(0), a_2(0)) = (0.2, 1.5)$, only configuration A is feasible initially. Suppose that sometime after starting from this initial condition, say $t = 3.5$, a fault is detected in configuration A and it becomes necessary to switch to either configuration B or C. Without using the switching rule of Eq. (21), it is not clear which of the two configurations should be activated at this time. Fig. 6b–c depict, respectively, the resulting closed-loop state and manipulated input profiles when configuration C is chosen. We see in this

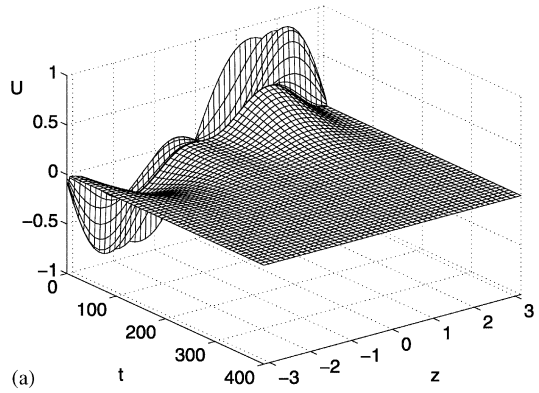


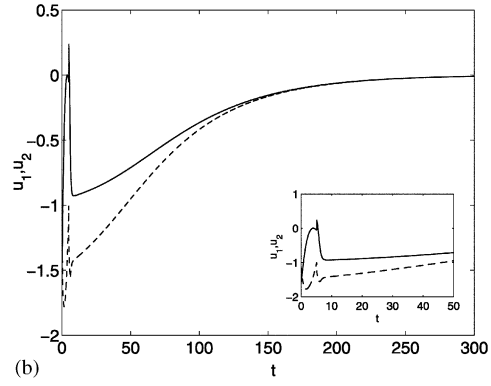


Fig. 7. (a) Closed-loop state profile (state feedback) for $(a_1(0), a_2(0)) = (0.2, 1.5)$ when configuration A fails at $t = 3.5$ and configuration B is activated. (b) Corresponding manipulated input profiles for $u_1$ (solid) and $u_2$ (dashed).

case that the controller is unable to stabilize the closed-loop system at the desired steady-state. This is expected since the state, at the time of switching, lies outside the stability region for configuration C (see point X on the solid trajectory in Fig. 6a). In contrast, by using the switching logic of the fault-tolerant control scheme proposed in Section 3, we conclude that it is configuration B, not C, that should be activated because the closed-loop trajectory at this time is inside the stability region of B (see dashed trajectory in Fig. 6a). Fig. 7 depicts the results for this case which show that the controller successfully stabilizes the closed-loop system when B is activated instead of C. The switching law, therefore, allows us to choose the appropriate actuator re-configuration scheme.

For the case of output feedback control, measurements from a pair of point sensors, located at $z_1 = 0.35\pi$ and $z_2 = 0.65\pi$, are used to obtain estimates of the first two eigenmodes. The estimates are then used in the implementation of the output feedback controller. Due to the slight discrepancy between the stability regions obtained under state and output feedback control (see Remark 7), the switching law proposed in Eq. (21) is used only as an approximate guide. The simulation results for this case are consistent with the state

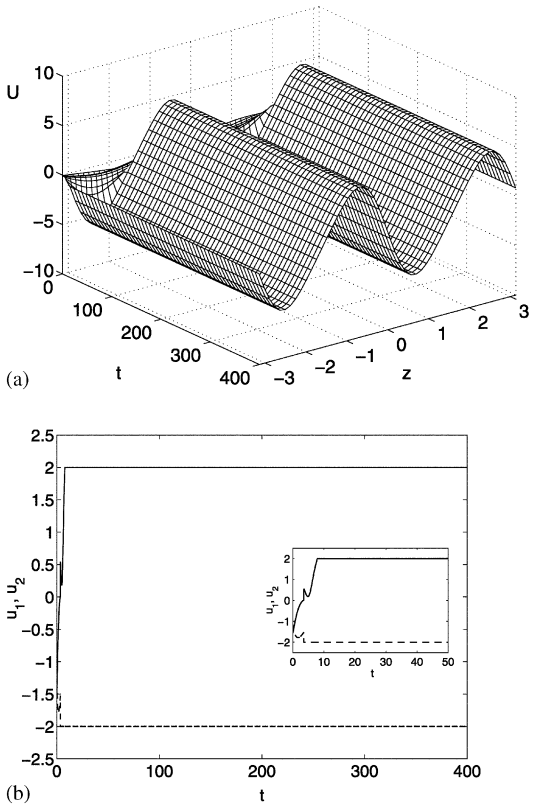


Fig. 8. (a) Closed-loop state profile (output feedback) for $(a_1(0), a_2(0)) = (0.2, 1.5)$ when configuration A fails at $t = 3.5$ and configuration B is activated. (b) Corresponding manipulated input profiles for $u_1$ (solid) and $u_2$ (dashed).

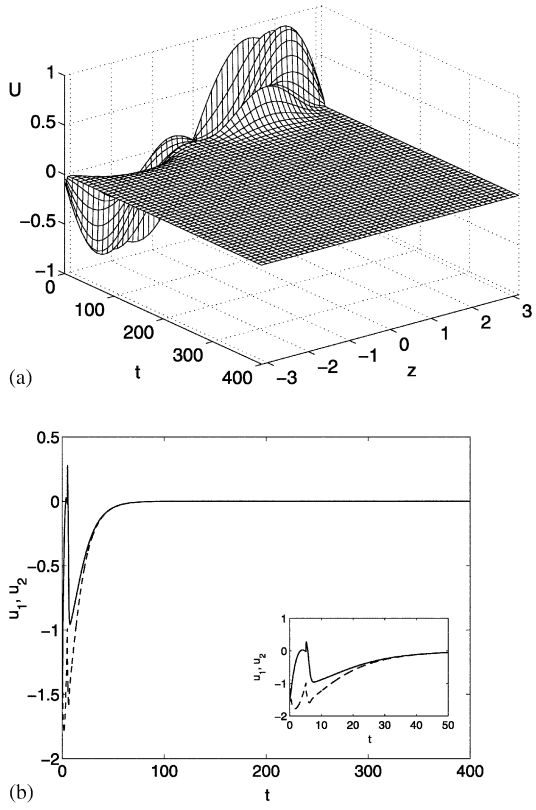


Fig. 9. (a) Closed-loop state profile (output feedback) for $(a_1(0), a_2(0)) = (0.2, 1.5)$ when configuration A fails at $t = 5$ and configuration B is activated. (b) Corresponding manipulated input profiles for $u_1$ (solid) and $u_2$ (dashed).

feedback results for both problems. We present only the results for the first problem. These are given in Figs. 8 and 9 which, respectively, show that the closed-loop system becomes unstable when configuration A fails at $t = 3.5$ and configuration B is activated, whereas closed-loop stability is maintained by activating configuration B when A fails at $t = 5.0$.

*Remark 8*. The fact that the fast stable modes were neglected in the controller design can result in some degradation in the control performance when the controller is implemented on the full (high-order) system. If these modes die out sufficiently fast, then such degradation will be minimal. However, since the control objective is to achieve stabilization of the PDE system, a second-order model that describes the evolution of the first two modes (which are unstable) was found to be sufficient to design a controller that stabilizes the zero solution of the KSE. Nonetheless, it is possible to enhance the performance further by keeping more modes in the reduced-order model in order to obtain a better approximation of the full system.

*Remark 9*. It should be noted that, while the KSE was used in this paper to demonstrate the design and implementation of the proposed fault-tolerant control scheme, the proposed approach can also be applied to other dissipative PDEs that can model fluid dynamic systems, such as the Burger's equation (Baker, Armaou & Christofides, 2000), the Korteweg–de Vries Burgers equation (Armaou & Christofides, 2000) and various forms of the Navier–Stokes equations (such as equations that describe two-dimensional transitional flow in a channel (e.g. see Baker et al., 2000)).

## 5. Conclusions

A fault-tolerant control system design methodology was proposed for fluid dynamic systems modeled by highly-dissipative PDEs with constrained control actuators. The central idea of the proposed method is that of coordinating feedback controller synthesis and switching between multiple, spatially-distributed control actuator configurations. Using appropriate finite-dimensional approximations of the PDE system, a stabilizing feedback controller was designed for a given actuator configuration, and an explicit characterization of the constrained stability region was obtained. Switching laws were then derived, on the basis of these stability regions, to orchestrate the transition between the control

actuator configuration, in a way that guarantees constraint satisfaction and preserves closed-loop stability of the infinite-dimensional system in the event of actuator failures. The results were applied to the problem of suppressing wave formation in falling liquid films via the stabilization of the zero solution of the one-dimensional KSE, with periodic boundary conditions, subject to actuator constraints and failures.

## Acknowledgements

Financial support, in part by UCLA through a Chancellor's Fellowship for Nael H. El-Farra, by the National Science Foundation, CTS-0129571, and by a 2001 Office of Naval Research Young Investigator Award is gratefully acknowledged.

## References

Armaou, A., & Christofides, P. D. (2000). Wave suppression by nonlinear finite-dimensional control. *Chemical Engineering Science 55*, 2627–2640.

Baker, J., Armaou, A., & Christofides, P. D. (2000). Nonlinear control of incompressible fluid flows: application to Burgers' equation and 2d channel flow. *Journal of Mathematical Analysis and Applications 252*, 230–255.

Bemporad, A., & Morari, M. (1999). Control of systems integrating logic, dynamics and constraints. *Automatica 35*, 407–427.

Chen, L. H., & Chang, H. C. (1986). Nonlinear waves on liquid film surfaces-II. Bifurcation analyses of the long-wave equation. *Chemical Engineering Science 41*, 2477–2486.

Christofides, P. D. (2001). *Nonlinear and robust control of PDE systems: methods and applications to transport-reaction processes*. Boston: Birkhäuser.

Christofides, P. D., & Armaou, A. (2000). Global stabilization of the Kuramoto–Sivashinsky equation via distributed output feedback control. *Systems and Control Letters 39*, 283–294.

El-Farra, N. H., & Christofides, P. D. (2003a). Hybrid control of parabolic PDEs: handling faults of constrained control actuators. In O. Maler & A. Pnueli (Eds.), *Lecture notes in computer science series*, vol. 2623 (pp. 172–187). Berlin: Springer.

El-Farra, N. H., & Christofides, P. D. (2003b). Bounded robust control of constrained multivariable nonlinear processes. *Chemical Engineering Science 58*, 3025–3047.

El-Farra, N. H., & Christofides, P. D. (2003c). Coordinated feedback and switching for control of hybrid nonlinear processes. *American Institute of Chemical Engineering Journal 49*, 2109–2123.

El-Farra, N. H., & Christofides, P. D. (2003d). Coordinated feedback and switching for control of spatially-distributed processes. *Computers and Chemical Engineering*, in press.

Greene, J. M., & Kim, J. S. (1988). The steady-states of the Kuramoto–Sivashinsky equation. *Physica D 33*, 99–120.

Hooper, A. P., & Grimshaw, R. (1985). Nonlinear instability at the interface between two viscous fluids. *Physics of Fluids 28*, 37–45.

Hu, C. B., & Temam, R. (2001). Robust control of the Kuramoto–Sivashinsky equation. *Dynamics of Continuous Discrete and Impulsive Systems-Series B-Applications and Algorithms 8*, 315–338.

Kevrekidis, I. G., Nicolaenko, B., & Scovel, J. C. (1990). Back in the saddle again: a computer assisted study of the Kuramoto–Sivashinsky equation. *SIAM Journal of Applied Mathematics 50*, 760–790.

Kobayashi, T. (2002). Adaptive stabilization of the Kuramoto–Sivashinsky equation. *International Journal of System Science 33*, 175–180.

Kuramoto, Y., & Tsuzuki, T. (1976). Persistent propagation of concentration waves in dissipative media far from thermal equilibrium. *Progress in Theoretical Physics 55*, 356–360.

Liberzon, D., & Morse, A. S. (1999). Basic problems in stability and design of switched systems. *IEEE Control Systems Magazine 13*, 59–70.

Lin, Y., & Sontag, E. D. (1991). A universal formula for stabilisation with bounded controls. *Systems and Control Letters 16*, 393–397.

Liu, W. J., & Krstic, M. (2001). Stability enhancement by boundary control in the Kuramoto–Sivashinsky equation. *Nonlinear Analysis: Theory, Methods and Applications 43*, 485–507.

Sivashinsky, G. I. (1980). On flame propagation under conditions of stoichiometry. *SIAM Journal of Applied Mathematics 39*, 67–82.

Temam, R. (1988). *Infinite-dimensional dynamical systems in mechanics and physics*. New York: Springer.